Performance Comparison of Four Commercial GE Discovery PET/CT Scanners: A Monte Carlo Study Using GATE

Original Article

Parham Geramifar[1,3,4], Mohammad Reza Ay[2,3,4], Mojtaba Shamsaie Zafarghandi[1], George Loudos[5], Arman Rahmim[6]

[1]Faculty of Nuclear Engineering and Physics, Amir Kabir University of Technology, [2]Department of Medical Physics and Biomedical Engineering, [3]Research Center for Science and Technology in Medicine, [4]Research Institute for Nuclear Medicine, Tehran University of Medical Sciences, Tehran, Iran
[5]Department of Medical Instruments Technology, Technological Educational Institute, Athens, Greece
[6]Department of Radiology, School of Medicine, Johns Hopkins University, Baltimore, USA.

(Received 17 August 2009, Revised 16 October 2009, Accepted 22 October 2009)

ABSTRACT

Combined PET/CT scanners now play a major role in medicine for in vivo imaging in oncology, cardiology, neurology, and psychiatry. As the performance of a scanner depends not only on the scintillating material but also on the scanner design, with regards to the advent of newer scanners, there is a need to optimize acquisition protocols as well as to compare scanner performances on an objective basis. In this study we evaluate and compare the performance of 4 Commercial GE PET/CT cameras, the (i) BGO-based Discovery LS PET/CT (DLS), (ii) the BGO-based Discovery ST PET/CT (DST), (iii) the BGO-based Discovery STE PET/CT (DSTE) and finally (iv) the LYSO-based Discovery RX PET/CT (DRX) scanner using the Geant4 Application for Tomographic Emission (GATE). GATE is an open source Monte Carlo simulation platform developed for PET and SPECT studies and is supported by the OpenGATE collaboration. In accordance with the National Electrical Manufactures Association (NEMA) NU 2-2001 protocols, the validation of models is carried out against actual published measurements and the performance comparison is done for sensitivity, scatter fraction and count rate performance, showing very similar performance compared with published results, thus enabling investigations to better model system performance (e.g. resolution degradation) within the reconstruction task.. The simulated results demonstrate highest sensitivity performance with the DST (though with the highest scatter fraction), and highest NECR performance for the LYSO-based DRX, The results also show that DRX, DLS and DSTE PET/CT cameras have nearly the same amount of scatter fraction.

Key Words: Positron emission tomography (PET), Scanner performance, GATE.

Iran J Nucl Med 2009;17(2):26-33

Corresponding author: Dr Mohammad Reza Ay, Department of Medical Physics and Biomedical Engineering, Tehran University of Medical Sciences, Tehran, Iran.
E-mail: mohammadreza_ay@tums.ac.ir

INTRODUCTION

Combined positron emission tomography and computed tomography (PET/CT) scanning now plays a major role in medicine for in vivo imaging in oncology, cardiology, neurology, psychiatry, and is considered as a major advance in imaging technology and patient care. The recent introduction of PET/CT scanners using fast scintillator detectors (e.g. LYSO) has made it possible to perform total body scans in shorter periods than with former scanners (e.g. BGO based), as a result of the shorter decay time and higher light output of LSO. As the performance of a scanner depends not only on the scintillating material but also on the scanner design, with regards to the advent of newer scanners, there is a need to optimize acquisition protocols as well as to compare scanner performances on an objective basis. The aim of this study was to evaluate and compare the performance characteristics of the PET components of 4 Commercial GE PET/CT cameras, namely (i) the BGO-based Discovery LS PET/CT (DLS), (ii) the BGO-based Discovery ST PET/CT (DST), (iii) the BGO-based Discovery STE PET/CT (DSTE) and finally (iv) the LYSO-based Discovery RX PET/CT (DRX) scanners using the Geant4 Application for Tomographic Emission (GATE). By validating the GATE models, we also demonstrate the flexibility and accuracy of GATE besides showing the potential benefits of a validated PET scanner simulation in design optimization and performance prediction.

METHODS

Monte Carlo Simulation

Full scanners simulations are based on the GATE toolkit which is an open source Monte Carlo simulation platform developed for PET and SPECT studies and is supported by the OpenGATE collaboration (1). The GATE Monte Carlo package is designed to simulate PET and SPECT systems and provides the ability to model and characterize the effects of photon non-collinearity, off-axis detector penetration, detector size and response, positron range, photon scatter, and patient motion on the resolution and quality of PET images (2, 3). It is an open-source extension of the GEANT4 Monte Carlo toolkit and the ROOT object oriented data analysis framework. The most advantageous features are its broad international support and the well validated and constantly updated underlying physics data and algorithms. Thus, as new features and refinements become available they are easily linked to GATE allowing it to continually expand and improve in order to meet rising technological demands and to incorporate new capabilities. GATE uses combinations of simple shapes (e.g., boxes, spheres, and cylinders), as defined in GEANT4 to generate complex geometric structures (4). The software's limitations with regard to generating adequately complex shapes are well within the tolerance and design of these scanners. GATE has the ability to convert photon interactions into counts in a manner analogous to that of a real scanner's detectors and electronics. This is accomplished in GATE by a series of signal processing chains, including the digitizer. Each module of the digitizer mimics a separate portion of a scanner's signal processing chain. The crystal QE, crystal blurring, thresholder, upholder, dead time and other electronics delay are defined in this module.

To mimics the effect of limited transfer rate, a module allows to simulate the data loss due to an overflow of a memory buffer, limited bandwidth of wires or buffer capacities of the I/O interfaces. The software's limitations with regard to generating adequately complex shapes are well within the tolerance and design of these scanners.

Simulated Scanners

The aforementioned cameras simulated in this work are utilizing the block design technology, where each block is an array of many crystals. The crystal dimensions are 4x8x30 mm3 for the DLS, 6.25x6.25x30 mm3 for the DST, 4.7x6.3x30 mm3 for the DSTE and 4.2x6.3x30 mm3 for the DRX, in transaxial, axial, and radial directions, respectively. There are 18 rings with 672 BGO crystals per ring in the DLS, 24 rings with 420 BGO crystals per ring in the DST, 24 rings with 560 BGO crystals per ring in the DSTE and 24 rings with 630 LYSO crystals per ring in the DRX. The DLS scanner has the largest ring diameter of 92.7 cm compared to 88.6 cm for the DST, DSTE and DRX scanners. Furthermore, the DLS has smaller axial and transaxial FOVs of 15.2 cm and 55 cm, respectively, compared to the axial FOVs of 15.7 cm and 70 cm for the other 3 scanners. The coincident window width is 12.5 ns for the DLS, 11.7 ns for the DST, 9.75 ns for the DSTE and 5.85 ns for the DRX. The lower energy threshold is set to 300 keV for the DLS model, 375 keV for the DST model and 425 keV for both the DSTE and DRX models. Furthermore, the upper energy threshold is set 650 keV for all four cameras.

Model Description

Model geometry and data acquisition system are the same for the aforementioned cameras, as all of them are utilizing the block design technology. In this section, model geometry, signal processing chain and simulation setup are described in detail.

A) Geometry

GATE uses combinations of simple shapes (e.g., boxes, spheres, and cylinders, as defined in GEANT4) to generate complex geometric structures. In accordance with the real scanners, the GATE model utilized for the PET components of these cameras was that of a cylindricalPET scanner system. The System which is a key-concept of GATE, provides a template of a predefined geometry to simulate a scanner. The geometrical volumes containing crystals are grouped in matrices, themselves assembled in submodules and modules. In accordance with the real scanners, 18 rings with 672 BGO crystals per ring in the DLS, 24 rings with 420 BGO crystals per ring in the DST, 24 rings with 560 BGO crystals per ring in the DSTE and 24 rings with 630 LYSO crystals per ring in the DRX were modeled. The shielding and packing materials within the detector blocks and the shielding surrounding the scanner rings are also accounted for in the model. The phantoms are modeled separately using the dimensions and tolerances as described in the published NEMA standards (5).

B) Signal Processing

The data collection system within GATE enables the modeling of the signal processing chain that is analogous to that of a real PET scanner. GATE also has the ability to convert photon interactions into counts in a manner analogous to that of a real scanner's detectors and electronics. This is accomplished in GATE by a series of signal processing routines known collectively as the digitizer. A sequence of digitizer modules to simulate the complete signal processing chain was used in the simulation (figure 1).

This sequence begins with the *Adder* module which integrates the energy deposition of a particle interacting within a single crystal. Next, the *Readout* module integrates the results from the *Adder* module within a block of crystals to create a pulse. Then a *Blurring* module applies a detection efficiency factor. Next, a *Deadtime* module is inserted to create deadtime at the Block level that is triggered by the pulses within a block. Following this, another *deadtime* module is applied at the Module level of the scanner to account for the multiplexor processing of the single events. An energy-window discriminator is then applied via the

Thresholder and *Upholder* modules. Finally, the remaining pulses are sorted by the *Coincidence* module. The coincident window width is 12.5 ns for the DLS, 11.7 ns for the DST, 9.75 ns for the DSTE and 5.85 ns for the DRX. The lower energy threshold is set to 300 keV for the DLS model, 375 keV for the DST model and 425 keV for both the DSTE and DRX models. Furthermore, the upper energy threshold is set 650 keV for all four cameras.

C) Simulation Setup

In accordance with the National Electrical Manufactures Association (NEMA) NU 2-2001 (NU01) protocols (5), the validation of models is carried out against actual published measurements and the performance comparison is done for sensitivity, scatter fraction and count rate performance. As specified by NEMA, six concentric aluminum tubes all 700 mm in length were simulated to detect camera sensitivity. A line source with 16 MBq of ^{18}F was placed in the innermost tube, a fillable polyethylene tube with inside diameter of 1 mm and outside diameter of 3 mm. The SF and counting rate measurements were performed using the NEMA scatter phantom: a 70 cm-in-length cylindrical tube with an outside diameter of 20.3 cm and a 6.4 mm hole size at an offset distance of 4.5 cm. The 80 cm line source is placed in the hole with different activities. In all the simulations the acquisition time of 10 seconds was selected.

RESULTS AND DISCUSSION

Overall robustness verification

While the GATE Monte Carlo package has been extensively validated, we performed overall robustness checks for the code for the cases of estimating axial sensitivity (3D), axial and transaxial detection position, gamma non-collinearity angle distribution (deg) and positron annihilation distance (mm). Because of the limited space, only the results for DRX are mentioned here.

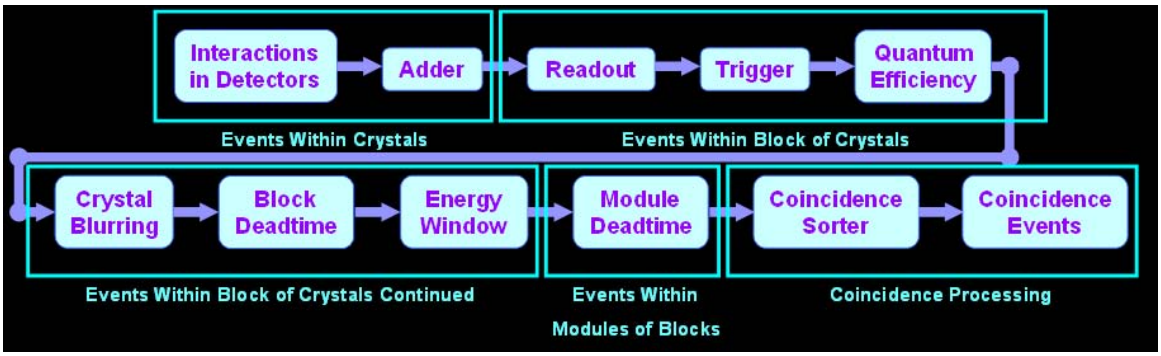

Figure 1. Signal processing chain simulated by GATE used to convert the particle interactions into coincidence counts.

Figure 2 illustrates the axial sensitivity (3D) of the DRX scanner. The 3D sensitivity is not uniformly distributed axially and falls off rapidly as one approach the edges of the axial FOV.

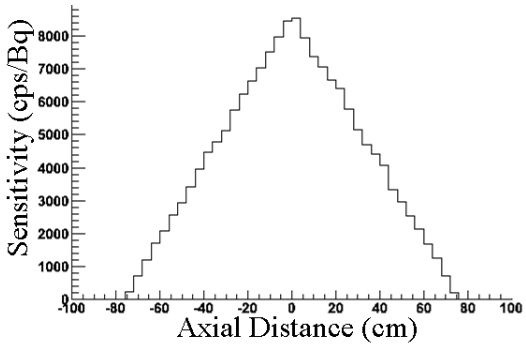

Figure 2. The DRX sensitivity as a function of axial position. The measurement is taken by applying a 5.85 ns timing window and a 425 -650 keV energy window.

Figure 3 shows the transaxial detection position which is a 2D histogram of the X and Y coordinates of the annihilation photons in the DRX detector rings. The distribution of detection is completely homogeneous.

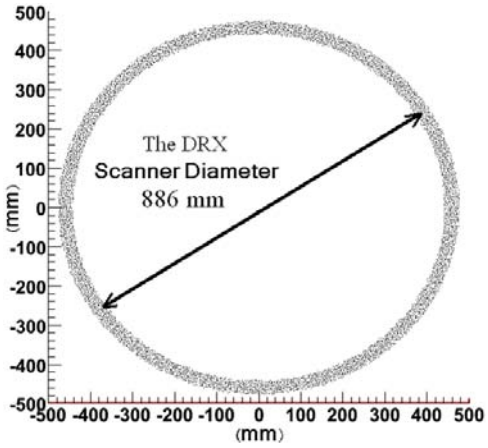

Figure 3. The DRX transaxial detection position in x-y plane.

The DRX axial detection position is shown in figure 4. It is a 1D histogram of the Z coordinate of detected annihilation photons. It illustrates the behavior of the detectors in axial direction. The histogram drops in inactive areas.

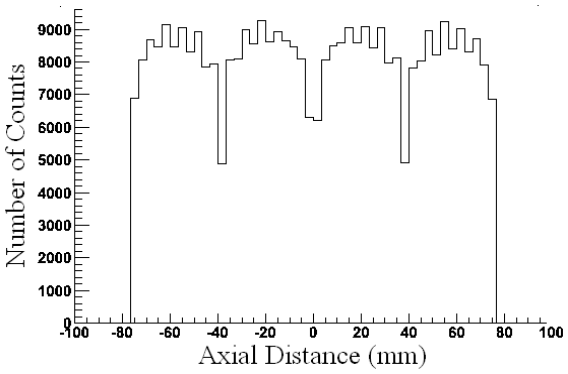

Figure 4. The DRX axial detection position. The histogram drops in inactive areas.

Finally, positron annihilation distance was characterized, as shown in figure 5 depicting the number of ^{18}F positrons as a function of their annihilation distance. Most of the positrons annihilate in distances less than 0.5 mm while a few annihilate in distances more than 1 mm.

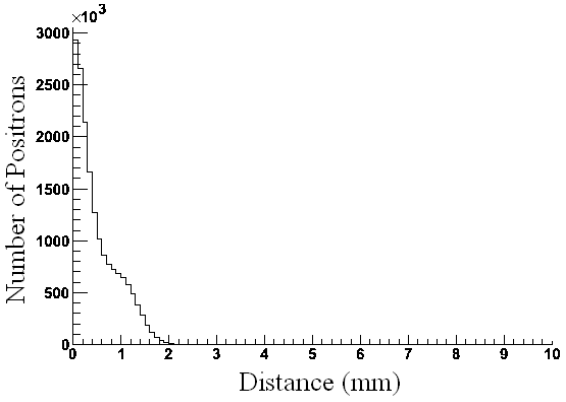

Figure 5. Positron annihilation distance for ^{18}F. The result is in good agreement with experimental value.

Validation by comparison

The codes were validated via comparison with published measured data for NU01 measurements test of these four GE scanners (6-9). The results are compared to published data for the sensitivity, scatter fraction and count rates. A comparison of the sensitivity of the GATE simulations to experimental values is presented in table 1. GATE data is presented with efficiency correction. Quantum efficiency (QE) is applied to individual events within the blocks in the digitizer and varied as a free parameter until the best agreements with experimental results were obtained.

A comparison of the scatter fraction results of the GATE simulations to those of the measured data (table 2) shows that the simulation's scatter fractions are very close to the measured values (within 1% to 4.5%). DST has the greater scatter fraction compared to the DLS, DSTE and DRX scanners.

The count rate performance for trues, randoms, and noise equivalent counts without randoms subtraction for each PET scanner are shown in figure 6. The random event rates were divided by a factor of 5 to enable both rates to be shown in one figure.

The noise equivalent count rate without randoms subtraction is calculated via $NECR= T^2/(T+S+R)$; where T, S, and R are the true, scatter, and random count rates, respectively. The simulated peak of true count rates and NECR curves are very close to the published measurements.

In figure 2, the increase in 3D sensitivity is due to the increase in the effective geometrical solid angle covered by the scanner. In 3D mode, as the increase in the number of LORs depends on the number of crystal rings, there is a much stronger variation in sensitivity, which peaks in the center of the axial FOV.

The homogeneity of the distribution in figure 3 shows the isotropic radiations besides the uniformity of detection. Behavior of the detectors in axial direction is shown in figure 4. As a matter of fact, the DRX has 4 modules of crystals in the axial direction and therefore 3 layers of packing material has been used between them, thus no counts should be detected in those inactive areas. However, due to the scatter and the LOR mispositioning, the axial position of the corresponding LORs is improperly histogrammed in those areas.

Table 1. Comparison of 3D sensitivity measurements between the GE Discovery PET\CT scanners and the GATE simulations.

Radial position (cm)	DLS published data [6] (cps/kBq)	DLS GATE Model (cps/kBq)	DST published data [7] (cps/kBq)	DST GATE Model (cps/kBq)	DSTE published data [8] (cps/kBq)	DSTE GATE Model (cps/kBq)	DRX published data [9] (cps/kBq)	DRX GATE Model (cps/kBq)
R0 = 0	6.41	6.54	9.118	9.23	8.8	8.43	7.30	7.36
R10 = 10	6.56	6.70	9.309	9.36	8.9	8.68	7.54	7.55
Ratio R0 / R10	0.977	0.976	0.979	0.986	0.988	0.971	0.968	0.974

Table 2 Comparison of 3D scatter fraction measurements between the GE Discovery PET\CT scanners and the GATE simulations.

DLS published data [6]	DLS GATE Model	DST published data [7]	DST GATE Model	DSTE published data [8]	DSTE GATE Model	DRX published data [9]	DRX GATE Model
42.85%	40.9%	45%	46%	33.9%	35.8%	31.8%	33.2%

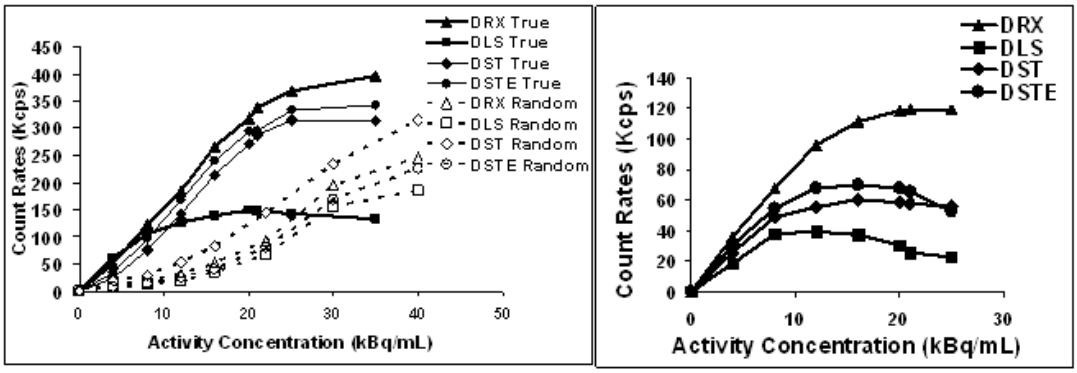

Figure 6. Random and True rates vs. activity concentration (left). NECR vs. activity concentration for GE PET cameras (right).The object imaged was the NEMA 2001 scatter phantom. The random event rates were divided by a factor of 5 to enable both rates shown in one figure.

The distribution of ^{18}F positron annihilation distances, as the result of figure 5, is in good agreement with published measure data by Sánchez-Crespo et al (10).

CONCLUSION

The obtained results demonstrate that all four PET cameras possess high NECR, low scatter fraction and acceptable sensitivity. However, there were some differences in their performances as we have especially assessed by the NECR concept. The GE Discovery PET/CT camera, DRX, was seen to out-perform the other three scanners in terms of overall NECR performance: This was due to having the highest true count performance, while having the lowest scatter fraction and an average random rate performance. Aside from the DRX, the DSTE was seen to outperform the DST and DLS scanners in terms of NEC better than the other cameras. Having successfully simulated the aforementioned four scanners, our research goal is to use the Monte Carlo simulation technique to better understand system performance, particularly with regards to resolution degrading phenomenon, and as such to arrive at powerful, accurate and feasible reconstruction algorithms with better knowledge of the available systems.

ACKNOWLEDGEMENTS

This work has been supported by the Research Center for Science and Technology in Medicine, Tehran University of Medical Sciences.

REFERENCES

1. OpenGATE Collaboration, GATE Users Guide, URL: http://opengatecollaboration.healthgrid.org
2. Buvat I, Lazaro D. Monte Carlo simulations in emission tomography and GATE: An overview. Nucl Instr Meth A. 2006;569:323-329.
3. Assue K, Breton V, Buvat I, Comtat C, Jan S, Kriegueld M et al. Monte Carlo simulation in PET and SPECT instrumentation using GATE. Nucl Instr Meth Phys Res A. 2004;527:180-189.
4. Strulab D, Santin G, Lazaro D, Breton V, Morel C. GATE (Geant4 application for tomographic emission): A PET/SPECT general purpose simulation platform. Nucl Phys B (Proc Suppl). 2003;125:75–79.
5. NEMA standards publication NU 2-2001: Performance measurements of positron emission tomographs, Technical report. Washington DC: National Electrical Manufactures Association; 2001.
6. Schmidtlein CR, Kirov AS, Nehmeh SA, Erdi YE, Humm JL, Amols HI et al. Validation of

GATE Monte Carlo simulations of the GE Advance/Discovery LS PET scanners. Med Phys. 2006;33(1):198-208.

7. Mawlawi O, Podoloff DA, Kohlmyer S, Williams JJ, Stearns CW, Culp RF et al. Performance characteristics of a newly developed PET/CT scanner using NEMA standards in 2D and 3D modes. J Nucl Med. 2004;45(10):1734-1742.

8. Teräs M, Tolvanen T, Johansson JJ, Williams JJ, Knuuti J. Performance of the new generation of whole-body PET/CT scanners: Discovery STE and Discovery VCT. Eur J Nucl Med Mol Imaging. 2007;34(10):1683-1692.

9. Kemp BJ, Kim C, Williams JJ, Ganin A, Lowe VJ; National Electrical Manufacturers Association (NEMA). NEMA NU 2-2001 performance measurements of an LYSO-based PET/CT system in 2D and 3D acquisition modes. J Nucl Med. 2006 Dec;47(12):1960-1967.

10. Sánchez-Crespo A, Andreo P, Larsson SA. Positron flight in human tissues and its influence on PET image spatial resolution. Eur J Nucl Med Mol Imaging. 2004;31(1):44-51.